Filtration Effects Due to Bioassay Cage Design and Screen Type

Author(s): Bradley K. Fritz, W. Clint Hoffmann, Muhammad Farooq, Todd Walker, and Jane Bonds

			Form Approved OMB No. 0704-0188

Report Documentation Page

Form Approved
OMB No. 0704-0188

Public reporting burden for the collection of information is estimated to average 1 hour per response, including the time for reviewing instructions, searching existing data sources, gathering and maintaining the data needed, and completing and reviewing the collection of information. Send comments regarding this burden estimate or any other aspect of this collection of information, including suggestions for reducing this burden, to Washington Headquarters Services, Directorate for Information Operations and Reports, 1215 Jefferson Davis Highway, Suite 1204, Arlington VA 22202-4302. Respondents should be aware that notwithstanding any other provision of law, no person shall be subject to a penalty for failing to comply with a collection of information if it does not display a currently valid OMB control number.

1. REPORT DATE **2010**	2. REPORT TYPE	3. DATES COVERED **00-00-2010 to 00-00-2010**

4. TITLE AND SUBTITLE **Filtration Effects Due to Bioassay Cage Design and Screen Type**	5a. CONTRACT NUMBER
	5b. GRANT NUMBER
	5c. PROGRAM ELEMENT NUMBER
6. AUTHOR(S)	5d. PROJECT NUMBER
	5e. TASK NUMBER
	5f. WORK UNIT NUMBER

7. PERFORMING ORGANIZATION NAME(S) AND ADDRESS(ES) **Navy Entomological Center of Excellence,Box 43, Bldg 937,Jacksonville,FL,32212-0043**	8. PERFORMING ORGANIZATION REPORT NUMBER

9. SPONSORING/MONITORING AGENCY NAME(S) AND ADDRESS(ES)	10. SPONSOR/MONITOR'S ACRONYM(S)
	11. SPONSOR/MONITOR'S REPORT NUMBER(S)

12. DISTRIBUTION/AVAILABILITY STATEMENT
Approved for public release; distribution unlimited

13. SUPPLEMENTARY NOTES

14. ABSTRACT

The use of bioassay cages in the efficacy assessment of pesticides, application techniques and technologies is common practice using numerous cage designs, which vary in both shape and size as well as type of mesh. The objective of this work was to examine various cage shapes and mesh types for their filtration effects on air speed, spray droplet size, and spray volume. Reductions in wind speed and droplet size seen inside the cages were measured by placing cages in a low-speed wind tunnel at air speeds of 0.5 m/ sec, 1 m/sec, 2 m/sec, and 4 m/sec and cage face orientations (relative to the air stream) of 0u, 10u, 22.5u, and 45u. Reduction in spray volume inside a select number of cages was also evaluated under similar conditions. Generally, greater air speed reductions were seen at lower external air speeds with overall reductions ranging from 30% to 88%, depending on cage type and tunnel air speed. Cages constructed with screens of lower porosities and smaller cylindrical-shaped cages tended to provide greater resistance to air flow and spray volume. Overall, spray droplet size inside the cages was minimally reduced by 0?10%. There was a 32?100% reduction in concentration of the spray volume applied relative to that recovered inside the bioassay cages depending on the cage geometry and screening material used. In general, concentration reductions were greatest at lower air speeds and for cages with lower porosity screens. As a result of this work, field researchers involved in assessing the efficacy of vector control applications will have a better understanding of the air speed and spray volume entering insect bioassay cages, relative to the amount applied, resulting in better recommended application techniques and dosage levels.

15. SUBJECT TERMS

16. SECURITY CLASSIFICATION OF:			17. LIMITATION OF ABSTRACT	18. NUMBER OF PAGES	19a. NAME OF RESPONSIBLE PERSON
a. REPORT **unclassified**	b. ABSTRACT **unclassified**	c. THIS PAGE **unclassified**	**Same as Report (SAR)**	**12**	

FILTRATION EFFECTS DUE TO BIOASSAY CAGE DESIGN AND SCREEN TYPE[1]

BRADLEY K. FRITZ,[2] W. CLINT HOFFMANN,[2] MUHAMMAD FAROOQ,[3] TODD WALKER[3] AND JANE BONDS[4]

ABSTRACT. The use of bioassay cages in the efficacy assessment of pesticides, application techniques, and technologies is common practice using numerous cage designs, which vary in both shape and size as well as type of mesh. The objective of this work was to examine various cage shapes and mesh types for their filtration effects on air speed, spray droplet size, and spray volume. Reductions in wind speed and droplet size seen inside the cages were measured by placing cages in a low-speed wind tunnel at air speeds of 0.5 m/sec, 1 m/sec, 2 m/sec, and 4 m/sec and cage face orientations (relative to the air stream) of 0°, 10°, 22.5°, and 45°. Reduction in spray volume inside a select number of cages was also evaluated under similar conditions. Generally, greater air speed reductions were seen at lower external air speeds with overall reductions ranging from 30% to 88%, depending on cage type and tunnel air speed. Cages constructed with screens of lower porosities and smaller cylindrical-shaped cages tended to provide greater resistance to air flow and spray volume. Overall, spray droplet size inside the cages was minimally reduced by 0–10%. There was a 32–100% reduction in concentration of the spray volume applied relative to that recovered inside the bioassay cages, depending on the cage geometry and screening material used. In general, concentration reductions were greatest at lower air speeds and for cages with lower porosity screens. As a result of this work, field researchers involved in assessing the efficacy of vector control applications will have a better understanding of the air speed and spray volume entering insect bioassay cages, relative to the amount applied, resulting in better recommended application techniques and dosage levels.

KEY WORDS Bioassay cages, spray flux, spray filtration

INTRODUCTION

Evaluating the efficacy of insect vector control treatments relies on accurate measurements of both the amount of spray material applied and insect mortality within a treated area. Bioassay cages confine mosquitoes to specific spatial locations downwind of an application site permitting repeated and/or controlled assessments of insecticide and/or machine treatment efficacies, which provide a basis for pest management programs. Although measurements of the portion of spray material aloft is well documented (May and Clifford 1967, Miller 1993, Cooper et al. 1996, Fritz and Hoffmann 2008a, Bonds et al. 2009), the interaction of the bioassay cage with the ambient air stream and applied spray and the resulting insect dosage rates inside the cage are not understood. Reports have found that screen materials with larger porosities filtered less spray

material (Breeland 1970, Boobar et al. 1988, Barber et al. 2006).

Construction materials and geometry have also been found to affect the spray and air flow penetration into the cage (Breeland 1970, Boobar et al. 1988, Bunner et al. 1989, Hoffmann et al. 2008). Screens placed across any air flow provide a resistance restricting flow (Kosmos et al. 1993, Miguel 1998, Teitel 2009). Screens also have an efficiency with which they collect spray material that is a function of the screen characteristics, spray droplet spectrum, and air speed (Fox et al. 2004, Fritz and Hoffmann 2008a).

Boobar et al. (1988) found that confined mosquito mortality rates did not always correlate well with the observed parameters used to monitor wild mosquito populations and suggested that filtering of the spray via deposition onto the screen surfaces contributed to these inconsistencies. Boobar et al. (1988) also observed that the mortality data between cages with varying screen types could not be compared without accounting for the differing filtering effects. This can also be extended to screens of varying geometrical design and orientation to mean air flow based on results from Bunner et al. (1989).

Hoffmann et al. (2008) conducted a series of studies for 2 bioassay cage designs, one a flat disk, the other a cylinder. Air speed, spray droplet size, and spray concentrations were measured inside and outside the cages. The results showed that concentrations inside the cage ranged from 50% to 70% of those measured outside the cage.

However, the measured concentration data reported by Hoffmann et al. was not corrected for the collection efficiency (CE) of the sampler used, which would have differed for the external and internal samplers as a result of the reduced air speed inside the cage (May and Clifford 1967). The samplers used in this study were relatively large in diameter (0.6 cm) and, for the droplet spectrum sampled, had approximate CEs of 6% and 30% at 0.5 m/sec and 4 m/sec, respectively (calculated after Fritz and Hoffmann 2008a). Like many of the studies cited, Hoffmann et al. (2008) was limited in scope relative to the variety of cages tested.

Given the number of bioassay cages in use with multiple cage geometries and screen mesh types, there is a need to quantify these effects. The objectives of this study were to determine the influence of bioassay cages on the air speed, spray droplet size, and amount of spray material penetrating the cage under multiple air speeds and cage orientations relative to the mean air stream.

MATERIALS AND METHODS

Wind tunnel testing facility

The study was conducted in the United States Department of Agriculture, Agricultural Research Service (USDA-ARS) Aerial Application Technology research group's low-speed wind tunnel at College Station, Texas. The tunnel is a push system with dimensions of 1.2 × 1.2 × 9.8 m. Using an electronic variable speed control, tunnel air speed can be varied across a range of 0.5–6.5 m/sec. A gridded flow straightener positioned in the tunnel 0.75 m downwind of the fan outlet provides for smooth air flow within the tunnel.

Bioassay cages

A selection of 12 mosquito bioassay cages along with 2 prototype sand fly cages were selected for testing (Figs. 1 and 2). The sand fly cages are prototypes and were constructed using the cardboard bodies from the Navy Entomological Center of Excellence and Clarke cages with amber lumite screen (BioQuip Products, Rancho Dominguez, CA) in place of the normal screen materials (T-1721 tulle [Walmart], and T-310 tulle [Walmart], respectively). Prior to testing, cage geometries and screen mesh characteristics were measured using an image analysis system developed for sizing droplets deposited on water-sensitive papers (Hoffmann and Hewitt 2005). Macroscopic images were recorded for a section of each of the meshes placed over a dark background such that the mesh fibers and background were contrasting colors. The imaging
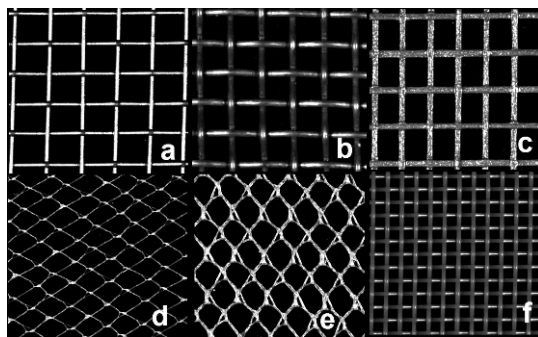

Fig. 1. Images of screening material tested: (a) aluminum screen, (b) copper screen, (c) fiberglass screen, (d) nylon tulle T-310, (e) nylon tulle T-1720, (f) amber lumite screen. Note: Screen pictures are not to scale.

system then converted image to black and white, with fibers being white against a black background. Mesh images were then analyzed for fiber diameter, distance between fibers, and percent open area. For each screen type the fiber diam, distance between fibers, hole percentage area, and porosity was measured across 40 unique locations and averaged (Table 1). Giving the multithread weave design of the T-310 and T-1721 tulle materials, additional characteristics were measured and recorded. Where the aluminum, copper, and fiberglass materials consist of single fibers in perpendicular crossing weaves, the 2 tulle fabrics consist of smaller diameter fibers in multithread, twisted interlocking perpendicular weaves, which result in less uniform screen structures (Figs. 1d, 1e). For these screens, single, double, and cluster fiber diam are reported along with distance between fibers, large- and small-hole percentage areas, and total porosity (Table 2).

General descriptions of cage construction and screen material and overall cage dimensions follow. The general descriptions follow the following format: Full cage name; abbreviated name using the format of a 3-letter abbreviation; XX (where XX is a numerical value equal to porosity of screen used); YZZ (where Y equals C [cylindrical cage] or D [disk cage] and ZZ is a numerical value equal to the diam [cm] of the disk or cylinder). The letters in the listing below correspond to those associated with the cages pictured in Fig. 2.

A. Naval Entomological Center of Excellence (NECE) Cage—NEC-74-D9: constructed from 237-ml Neptune paper cans. Screen material is T-1721 tulle (Walmart). Dimensions: 9 cm diam × 6 cm depth.

B. Kline Cage—KLI-59-C9: constructed from folded and stapled mesh screening. Screen material is plastic-coated fiberglass mesh (16 mesh). Dimensions: 20 cm × 9 cm diam
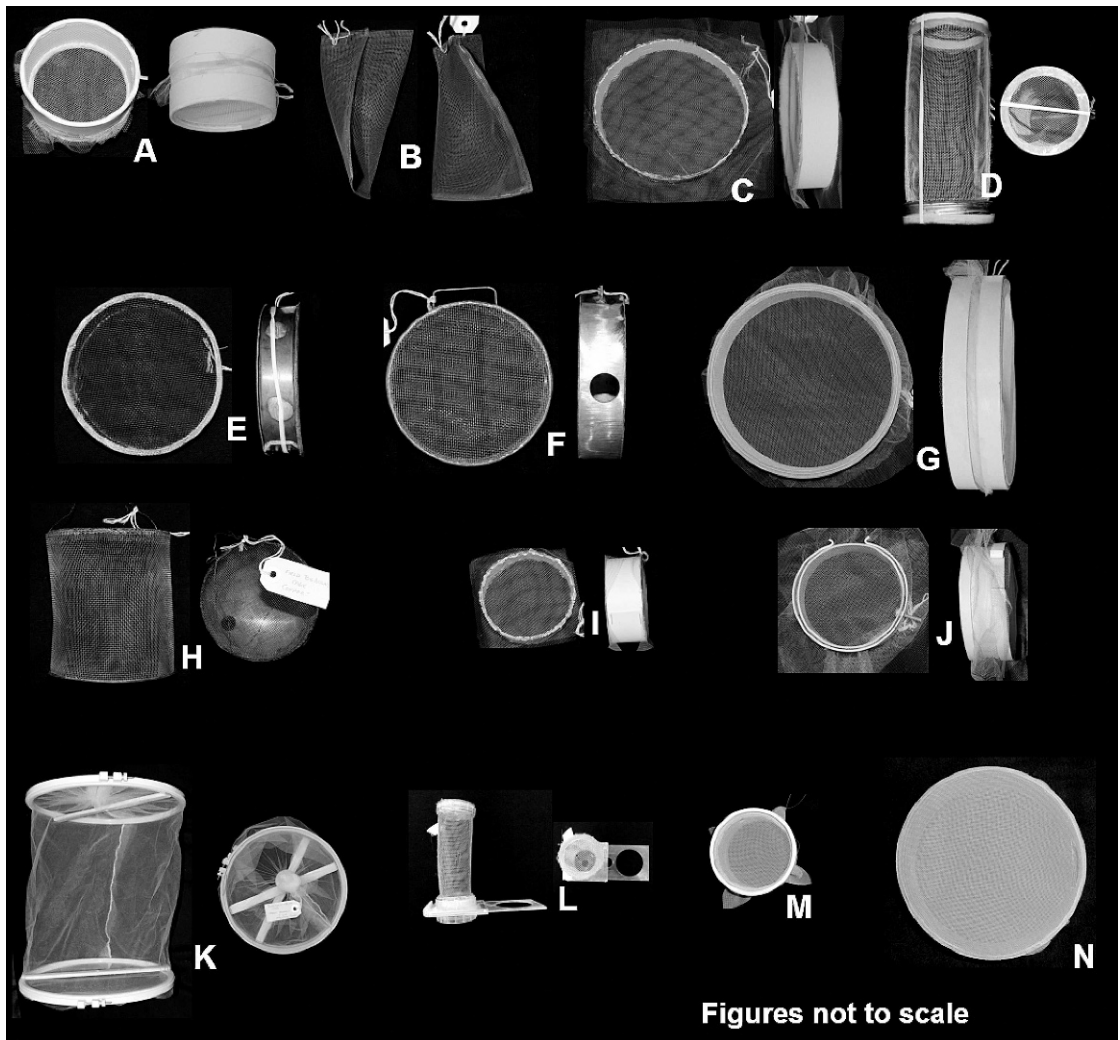
Fig. 2. Mosquito bioassay cages. A: NECE Cage—NEC-74-D9; B: Kline Cage—KLI-59-C9; C: Syke-Janousek Cage 1—SYJ-84-D17; D: Meisch Cage—MEI-72-C9; E: PHEREC Cage—PHE-58-D14; F: PHEREC Field Cage—PFC-72-D14; G: Clarke Cage—CLA-84-D16; H: PHEREC Field Bioassay—PFB-58-C12; I: Syke-Janousek Cage 1—SYJ-84-D9; J: DVEC Center PVC Cage—DVE-74-D11; K: Cooperband-Allan USDA Cage—CAU-84-C26; L: Chaskopoulou/WHO Cage—WHO-72-C5; M: NECE Sand fly Cage—NSC-47-D9; N: Clarke Sand fly cage—CSC-47-D16. NOTE: Cages M and N are adapted from the A and B cages, with original screening material replaced with amber lumite screen (BioQuip Products). Side views are not shown for these cages as they are the same as those shown for A and B.

(center) × 12 cm (ends). Note: Although this cage is defined here as a cylindrical cage, it is an irregular volume whose ends taper to a sharp edge.

C. Syke-Janousek Cage 1—SYJ-84-D17: constructed from cardboard ring with mesh glued to each face along the ring edge. Screen material is T-310 tulle (Walmart). Dimensions: 17 cm diam × 4 cm depth.

D. Meisch Cage—MEI-72-C9: constructed from screened plastic rings enclosing the ends of a cylinder constructed from metal screen. Screen material is 16-mesh aluminum win-

dow screen. Dimensions: 9 cm diam × 21 cm length.

E. Public Health Entomology Research and Education Center (PHEREC) Cage—PHE-58-D14: constructed from copper ring with copper screen soldered to each face. Screen material is copper mesh. Dimensions: 14 cm diam × 3.5 cm depth.

F. PHEREC Field Cage—PFC-72-D14: constructed from stainless steel ring with steel mesh welded to each face. Screen material is stainless steel mesh. Dimensions: 14 cm diam × 3.5 cm depth.

Table 1. Image analysis of mesh properties for single-weave materials.

Screen type	Fiber diam (mm)	Distance between fibers (mm)	Porosity (%)
Aluminum	0.26	1.7	71.7
Copper	0.48	2.0	57.9
Fiberglass	0.40	1.7	58.8
Amber lumite	0.26	0.81	46.6

G. Clarke Cage—cLA-84-D16: constructed from concentric, friction fit cardboard rings that secure screen material to each face. Screen material is T-310 tulle (Walmart). Dimensions: 16 cm diam × 4 cm depth.
H. PHEREC Field Bioassay Cage—PFB-58-C12: constructed from rigid screen material with solid copper bottom and screened top. Screen material is copper screen. Dimensions: 11.5 cm diam × 13.5 cm height.
I. Syke-Janousek Cage—1–SYJ-84-D9: cardboard ring with mesh glued to each face along the ring edge. Screen material is T-310 tulle (Walmart). Dimensions: 9 cm diam × 4 cm depth.
J. Disease Vector and Ecology Control (DVEC) Center PVC Cage—DVE-74-D11: constructed from PVC ring with secure clips formed from PVC ring strips. Screen material is T-1721 tulle (Walmart). Dimensions: 11 cm diam × 4 cm depth.
K. Cooperband–Allan United States Department of Agriculture (USDA) Cage—CAU-84-C26: constructed from screen material sewed into 26 mm diam cylindrical sleeve and held to shape using sewing rings at top and bottom. Screen material is T-310 tulle (Walmart). Dimensions: 26 cm diam × 32 cm length.
L. Chaskopoulou–World Health Organization (WHO) Cage—WHO-72-C5: constructed from WHO insecticide resistance test kits and screen secured into cylindrical shape with screened plastic cap on top end and plastic gate valve on bottom end. Screen material is 16-mesh aluminum window screen material. Dimensions: 4.5 cm diam × 12 cm length.
M. NECE Sand fly Cage—NSC-47-D9: constructed from 237-ml Neptune paper cans.

Screen material is amber lumite screen (BioQuip Products). Dimensions: 9 cm diam × 6 cm depth.
N. Clarke Sand fly cage—CSC-47-D16: constructed from concentric, friction-fit cardboard rings that secure screen material to each face. Screen material is amber lumite screen (BioQuip Products). Dimensions: 16 cm diam × 4 cm depth.

Air speed reduction testing was conducted on all 12 cages, and the spray volume penetration testing was conducted on 4 mosquito bioassay cages and the 2 prototype sand fly bioassay cages. The selected cages for the spray penetration testing from this list were A, E, G, L, M, and N.

Air speed reduction testing

The cages were mounted in the tunnel approximately 5 m downwind of the fan in the center of the cross-sectional area as shown in Fig. 3. Internal and external air speeds were measured simultaneously using 2 Kanomax Clinomaster (Model A533; Kanomax USA Inc., Andover, NJ) high-precision hot-wire anemometers (measurement range: 0.05–5.0 m/sec; resolution: 0.01 m/sec; accuracy: ±2% of reading or ±0.015 m/sec, whichever is greater). One anemometer was positioned within the center of each cage, and the other was positioned outside and upstream of the cage (approximately 10 cm) at the same height. The anemometers were inserted into the cages, from the bottom, either through an insect insertion hole or, if not available, an incision in the screen.

For each cage, 3 replicated measurements were made at 4 air speeds (0.5 m/s, 1 m/s, 2 m/s, and 4 m/s) and 4 orientations of the cage face relative to the mean air direction (0°, 10°, 22.5°, and 45°). The cages were mounted in a frame that allowed for rotation around the air speed probe. Air speed measurements were taken over a 30-s period, during which the instruments sampled in 1-s intervals. Average, maximum, and minimum air speeds were recorded for each replication. Averages and standard deviations were determined across each set of replications, and the percent reduction of internal versus external air speed was determined using Equation 1. Significance of air speed and cage orientation changes on the percent reduction of internal air speed was tested, using SYSTAT (v. 13.00.05, Systat Software,

Table 2. Image analysis results of mesh properties for multi-weave materials.

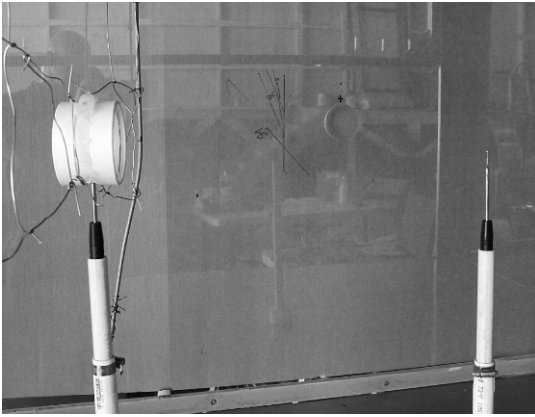| Screen type	Fiber diam (single/double/cluster) (mm)	Distance between fibers (mm)	Hole percent area (large/small) (%)	Porosity (%)
T-310 tulle	0.051/0.086/0.257	1.1	81.5/2.1	83.6
T-1721 tulle	0.12/0.30/0.40	1.4	71.7/2.6	74.3

Fig. 3. Hot-wire anemometer probes positioned for air speed measurements inside and outside of the Navy Entomological Center of Excellence (NECE) bioassay cage.

Chicago, IL) general linear model analysis at the alpha = 0.05 significance level:

$$\% \, Reduction = \left(1 - \frac{Airspeed_{inside \, cage}}{Airspeed_{outside \, cage}}\right) 100. \quad (1)$$

Droplet size testing

Droplet sizing measurements were made using a laser diffraction system (discussed below), which required an uninterrupted line of sight between the laser emission point and the receiving lens. To maintain this line of sight, 2 open-faced (front and rear openings) chambers spanning the tunnel were constructed. These chambers enclosed the distance between the laser outlet and the lens detector while allowing for screening materials to be attached over the front and back faces. One chamber was constructed with a flat face and the other with a rounded face (Fig. 4) to represent the 2 cage geometries tested. The chambers were mounted on a pivot to allow the frontal faces to be rotated to correspond with the same orientation angles selected for the air speed testing. Screening materials were secured in place using magnetic tape that adhered to metal strapping attached to the frame pinning the edges of the screen. This allowed screening materials to be replaced every 3 measurement replications to prevent material buildup on screens from affecting droplet sizing results.

For each of the bioassay cages selected, the corresponding screen type and frontal face shape (flat or round) was tested for droplet size within the screened area at 4 air velocities (0.5 m/s, 1 m/s, 2 m/s, and 4 m/s) and 4 frontal face orientations (0°, 10°, 22.5°, and 45°). Additionally, droplet size was measured with the chambers in place but with the screening material absent as a measure of droplet

size external to the cage. For all screen types, air velocity and orientation combinations, 3 replicated droplet size measurements were made.

A Sympatec HELOS laser diffraction droplet sizing system (Sympatec Inc., Clausthal, Germany) was used. The HELOS system uses a 623-nm He-Ne laser and was fitted with an R5 lens, resulting in a dynamic size range from 0.5 μm to 875 μm across 32 sizing bins. Tests were performed within the guidelines provided by ASTM Standard E1260: Standard Test Method for Determining Liquid Drop Size Characteristics in a Spray Using Optical Nonimaging Light-Scattering Instruments (ASTM, 2003). Droplet sizing data included volume median diam (D_{V50}), and the 10% and 90% diam (D_{V10} and D_{V90}) (ASTM E1620, 2004). D_{V50} is the droplet diam (μm), where 50% of the spray volume is contained in droplets of equal or lesser diam. D_{V10} and D_{V90} values are likewise the droplet diam, where 10% and 90% of the spray volume, respectively, is contained in droplets of equal or lesser diam. Averages and standard deviations were determined and recorded. Reductions in D_{V10}, D_{V50}, and D_{V90}, relative to the absence of the screening material, were also determined. Significance of air speed and face orientation was tested using general linear model analysis in SYSTAT (v. 13.00.05, Systat Software) at the alpha = 0.05 significance level.

Spray penetration testing

Spray penetration testing was conducted for the selected cage designs (as mentioned previously) at 0.5 m/sec, 2 m/sec, and, 4 m/sec tunnel air speeds and at 0° and 22.5° orientations (screen face relative to the mean tunnel air stream, with 0° being perpendicular to the wind direction). Five replication measurements were conducted for each cage/air speed/orientation combination. An additional air speed of 1 m/sec was examined for the 2 sand fly cages due to below-detection-threshold concentrations observed at the 0.5 m/sec air speed. For measurement of the spray penetration, the cages were mounted within the tunnel approximately 5 m downwind of the fan in the center of the cross-sectional area. Spray concentrations inside the cages were measured using small diameter stainless steel wire (0.56 mm thickness × 150 mm length) inserted into the cages from below through access holes (Fig. 5). Wires placed inside the cages were either bent in half or in thirds, depending on cage height, to accommodate fit. This was done, rather than using shorter wires, to maximize the sampling area due to the low spray concentrations being sampled. A second sampler was placed 0.5 m upwind and external to the cage to measure the concentration of spray material applied to the cage. The samplers were held using hemostats
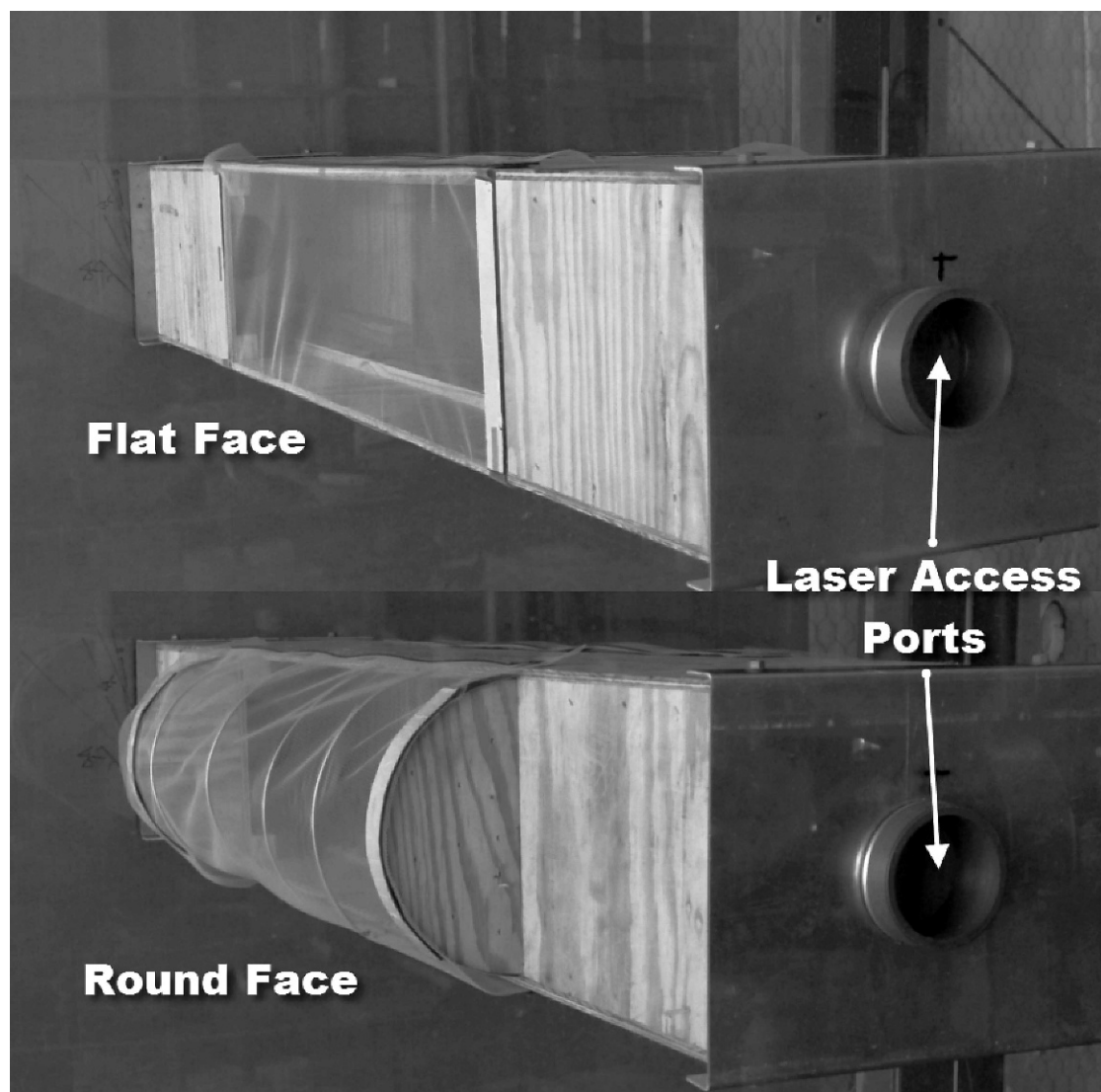
Fig. 4. Flat and round faces frames spanning wind tunnel walls for droplet sizing of spray penetration screen materials.

that were held in place in the tunnel on posts equipped with magnets.

After each replication, the samplers were collected and placed into individually labeled plastic bags and stored in an ice chest. Prior to placement of samplers, hemostats were cleaned in acetone and allowed to dry. New samplers were handled with a fresh set of gloves for preparation and placement to eliminate contamination. Test cages were replaced after 3 replications to minimize any possible bias from spray material buildup on the screens on spray penetration. Samples were processed in a laboratory by pipetting 15 ml of hexane into each bag, agitating the bags, and decanting 6 ml of the effluent into a cuvette. The cuvettes were then placed into a spectrofluorophotometer (Model RF5000U; Shimadzu, Kyoto, Japan) with an excitation wavelength of 372 nm and an emission at 427 nm and a minimum detection level of 0.00007 μg/cm². Fluorometric readings were converted to concentrations of spray material per area sampled using comparative analysis with fluorometric standards of known tracer dye concentration.

Prior to comparison of the cage internal and external spray concentrations, concentration data were corrected for the collection efficiency (CE) of the samplers. May and Clifford (1967) demonstrated that cylindrical collectors had CEs that varied with droplet size and air speed. The sampler CE values were calculated using the droplet spectrum and air speed data measured
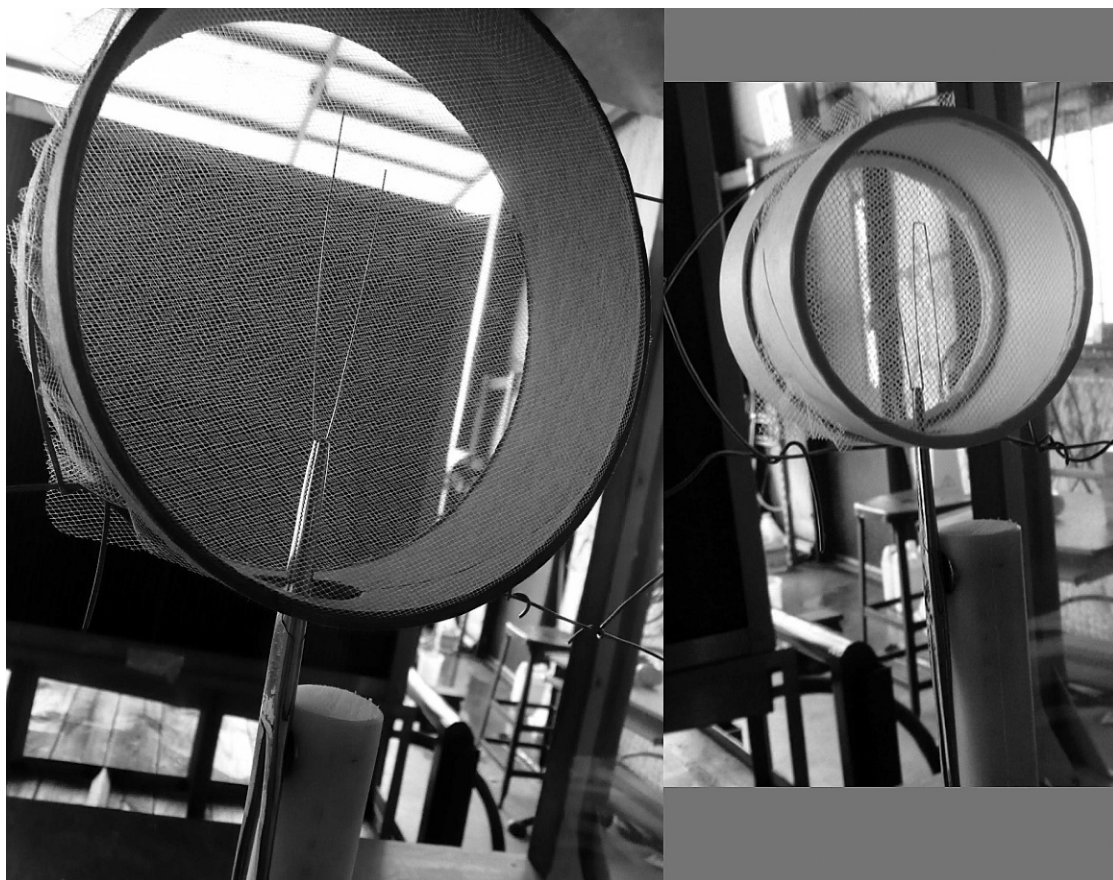
Fig. 5. Spray penetration measurement inside cages using stainless steel wire deposition samplers held in place using hemostats.

for each test condition following the methods outlined by Fritz and Hoffmann (2008a, 2008b). The droplet size spectrum data used to correct the internal and external samplers for CE were taken from measurements made for the different screening materials, air speeds, and orientations as discussed earlier. The external sampler CE calculation used the droplet size spectrum measured with no screen in place at the air speed being tested. The internal sampler CE calculation used the droplet size spectrum for the screen, air speed, and orientation angle associated with the cage and conditions being tested. For example, to correct measured concentration taken inside the NEC-74-D9 (NECE) cage at 2 m/s and 0° orientation, the droplet size spectrum measured for the T-1721 tulle at 2 m/s and 0° orientation was used. Air speed outside the cage was measured using a hot-wire anemometer (Model 407119A; Extech Instruments, Waltham, MA). The air speed data used in the CE calculations were calculated using the reduction levels measured as part of the air speed testing.

Internal ($C_{internal}$) and external ($C_{external}$) measured concentrations were then adjusted for CE, and the reduction in concentration determined using Equation 2. Significance of air speed and frontal face orientation was tested using SYSTAT (Systat Software) general linear model analysis at the alpha = 0.05 significance level:

$$Reduction\,(\%) = \left(1 - \frac{c_{internal}}{c_{external}}\right)100. \qquad (2)$$

Spray generation

The spray used in the droplet sizing and spray concentration studies was generated using an air-assisted dual-venturi-style, stainless steel nozzle (Advanced Special Technologies, Winnebago, MN), which produces a D_{V50} of 21.7 μm for oil sprays (Hoffmann et al. 2007). A BVA crop oil with Uvitex dye (BASF) added at a rate of 1 g/liter was metered to the nozzle using a syringe pump (NE-4000 Double Syringe Pump; New Era Pump Systems, Wantagh, NY). A total of 3 ml at a volume feed rate of 25 ml/min was used for each

Table 3. Air speed reductions by bioassay cage at each air speed and orientation and significance levels.

Cage[1]	Percent reduction (%) averaged within air speed across all orientations 0.5, 1, 2, 4 m/s	Significance (* if significant) Air speed	Significance (* if significant) Orientation
N: CSC-47-D16	87, 79, 74, 63	* ($P < 0.001$)	* ($P = 0.034$)
M: NSC-47-D9	80, 81, 76, 68	* ($P < 0.001$)	($P = 0.462$)
H: PFB-58-C12	70, 65, 58, 46	* ($P < 0.001$)	* ($P = 0.015$)
B: KLI-59-C9	66, 56, 51, 41	* ($P < 0.001$)	($P = 0.063$)
F: PFC-72-D14	65, 52, 46, 30	* ($P < 0.001$)	($P = 0.683$)
D: MEI-72-C9	63, 50, 43, 33	* ($P < 0.001$)	($P = 0.166$)
L: WHO-72-C5	57, 48, 40, 25	* ($P < 0.001$)	($P = 0.515$)
E: PHE-58-D14	57, 47, 42, 23	* ($P < 0.001$)	($P = 0.718$)
A: NEC-74-D9	57, 42, 34, 23	* ($P < 0.001$)	* ($P = 0.020$)
I: SYJ-84-D9	57, 39, 31, 19	* ($P < 0.001$)	($P = 0.749$)
C: SYJ-84-D17	52, 38, 30, 30	* ($P < 0.001$)	($P = 0.724$)
J: DVE-74-D11	52, 37, 29, 19	* ($P < 0.001$)	($P = 0.326$)
G: CLA-84-D16	51, 36, 26, 13	* ($P < 0.001$)	($P = 0.180$)
K: CAU-84-C26	38, 27, 19, 12	* ($P < 0.001$)	($P = 0.795$)

[1] Letter next to cage corresponds to picture of cage in Fig. 2.

spray replication. The air pressure to the nozzle was 552 kPa (80 psi).

RESULTS

Effect of cage design and orientation on air speed reductions

Mean internal air speed reductions, as determined by using Equation 1 for each external air speed and face orientation angle, and test of significance are presented in Table 3 based on an approximate order of magnitude from highest to lowest reduction in air speed. Only external air speed was a significant factor for the reduction observed inside each cage. Orientation was significant in 3 of the cages with cage shapes varying from flat disks to cylinders. All cages showed greater overall reductions at lower external air speeds. Generally, cages constructed of screening materials with lower porosities (i.e., copper, fiberglass, or amber lumite) tended to have greater reductions in air speed. There were strong linear relationships (R^2 = 0.74, 0.84, 0.87, and 0.74 for air speeds of 0.5 m/s, 1 m/s, 2 m/s, and 4 m/s, respectively) between porosity and air speed reduction, irrespective of cage design, for each external air speed tested. Generally disk-shaped cages tended to show lesser reductions, as compared with cylindrical cages, with the exception of the Cooperband–Allan USDA (CAU-84-C26) cage, which was due to its large diam and flexible, high-porosity (84%) screening material, presenting a relatively flat face to the oncoming air stream.

Table 4. Droplet size reduction for screening materials at multiple air speeds and orientation angles.

Air speed (m/s)	Orient. angle	Aluminum flat 10	Aluminum flat 50	Aluminum flat 90	Aluminum round 10	Aluminum round 50	Aluminum round 90	Copper flat 10	Copper flat 50	Copper flat 90	Copper round 10	Copper round 50	Copper round 90
0.5	0	4.8	3.4	1.9	2.1	1.9	0.8	3.7	5.5	5.3	2.1	1.5	0.5
0.5	10	3.7	3.2	1.6	8.8	5.9	3.0	4.8	4.6	3.1	1.6	0.4	−0.8
0.5	22.5	8.0	6.5	3.3	4.5	2.1	0.1	2.7	3.8	3.0	3.2	2.1	1.6
0.5	45	7.2	3.2	0.1	7.2	3.8	2.5	16.3	9.4	4.0	4.0	1.1	−0.1
1	0	11.8	8.3	4.8	9.3	5.3	2.8	10.8	9.2	7.0	9.5	6.3	4.1
1	10	8.0	5.3	2.9	9.5	6.8	4.3	12.0	10.5	9.7	11.8	7.4	3.6
1	22.5	12.3	7.9	4.0	13.0	7.5	3.3	13.5	10.3	7.0	11.5	6.8	3.3
1	45	11.8	7.4	3.3	15.5	9.0	4.3	16.7	12.5	8.0	13.5	7.5	3.6
2	0	4.1	7.8	6.3	2.5	7.4	6.9	−0.3	7.1	9.0	2.5	6.7	5.7
2	10	1.4	5.9	4.9	3.0	7.1	6.2	5.8	10.6	10.3	−1.9	3.9	4.2
2	22.5	1.9	6.5	5.1	6.6	8.9	5.8	5.8	10.8	10.6	5.5	7.6	5.1
2	45	8.8	10.0	7.0	7.7	8.3	5.4	6.5	10.2	8.1	12.9	10.9	6.1
4	0	−9.0	4.3	5.7	−6.4	6.2	7.7	−9.0	7.6	11.8	−4.8	6.4	7.2
4	10	−11.9	2.7	4.3	−12.5	3.1	6.1	−12.2	4.5	7.4	−8.3	3.9	4.7
4	22.5	−10.6	4.5	6.8	−6.1	3.7	3.7	−4.2	8.4	10.4	−10.6	3.1	6.2
4	45	−2.6	6.4	5.5	0.3	12.3	16.0	−5.8	9.2	13.4	−0.3	7.2	5.5

Droplet size reductions

Droplet size reduction levels are given for the different screening materials and face geometries at the different wind speeds and orientation angles in Table 4. Generally, screens with larger fiber diam and the lower porosity, such as the copper and fiberglass screens, had the highest reductions in the droplet size. Neither air speed nor orientation had a significant effect on D_{V50} values. Generally only air speed was a significant factor affecting the D_{V10} and D_{V90} values. Other than a few cases, face orientation was not significant. At lower air speeds, reduction in D_{V10}, D_{V50}, and D_{V90} values for all screen materials was lower than the reduction levels observed at the higher air speeds. Although D_{V90} reductions followed this trend at all air speeds, the overall D_{V50} reductions for all screens were less at 4 m/sec than at 1 m/sec and 2 m/sec air speeds. The D_{V10} values increased (negative percent reduction values) at the 4 m/sec air speeds.

The probability of impaction of droplets onto the screen surface at air speed with the largest droplets was reflected in the increased reductions measured for the Dv_{90} values at 4 m/sec. The probability of a droplet impinging on the screening fibers increases with air speed because the droplets entrained in the air stream also have increased velocities. Also, larger droplets have a higher probability of impinging on the screening fibers than smaller droplets. Therefore, at the higher air speeds, the larger droplets that make up the upper end of the spray distribution cumulative distribution curve are more likely to impinge on the screening fibers than the smaller droplets. When this occurs, the spray cloud inside the cage will be composed of those droplets not collected by the screening fibers. These reductions are similar to those observed by Hoffmann et al. (2008).

Collection efficiency

The correction for CE had significant impact on the overall calculated reduction of spray material penetrating the bioassay cages. The Clarke cage testing resulted in external and internal sampler CEs of 53% and 33% at 0.5 m/sec, and 81% and 79% at 4 m/sec, respectively. Correcting the sampler concentration data for sampler CE at 0.5 m/sec, the average spray concentration reduction inside the cage was 51% versus 68% (uncorrected data). Likewise, at 4 m/sec, average spray concentration reductions were 33% and 31%, with and without sampler CE correction, respectively. The same cage with amber lumite screen (Clarke sand fly cage) had internal and external sampler CEs of 58% and 22% at 1 m/sec air speed. Spray concentration reductions were 98% and 99%, with and without sampler CE correction, respectively. This correction was most significant for cages and air speeds with the greatest differential between internal and external air speeds.

Reduction of spray concentration inside cages

Data on observed spray concentration reductions are shown in Table 5. Analysis of the data showed no significant differences between replications ($\alpha = 0.05$ level). The orientation angle was not a significant factor for any of the cages. Therefore, the average reduction values presented in Table 5 are based on both the 0° and 22.5° orientation angle data. There was a very strong

Table 4. Extended.

| Reduction (%) in DvX where X is the 10%, 50%, or 90% volume | | | | | | | | | | | | | | | | | |
| Fiberglass flat | | | Fiberglass round | | | T-1721 flat | | | T-310 flat | | | T-310 round | | | Amber lumite flat | | |
10	50	90	10	50	90	10	50	90	10	50	90	10	50	90	10	50	90
5.3	4.8	2.9	2.7	2.1	1.1	−3.2	−1.1	0.1	−3.7	−2.1	0.3	4.8	3.6	1.6	8.9	6.6	3.7
1.6	2.1	1.8	4.8	3.8	1.8	2.9	1.7	0.1	−0.3	0.0	−0.3	4.3	3.1	1.1	5.4	6.0	5.4
6.1	4.8	2.6	7.5	4.6	1.4	6.9	3.8	0.4	−1.3	0.4	0.8	6.1	2.7	0.0	8.9	6.6	3.7
11.6	6.8	2.9	4.5	1.5	1.5	9.1	4.4	1.2	4.8	3.1	2.3	5.1	2.1	2.3	1.8	5.4	5.8
11.0	8.5	6.1	12.0	9.0	6.9	6.0	3.7	2.0	6.3	3.5	1.6	9.0	6.1	3.5	8.7	7.1	5.3
2.5	1.8	1.5	11.0	7.4	4.0	11.3	7.0	3.6	6.8	4.0	2.3	11.3	7.7	4.3	9.6	7.6	4.9
15.3	10.8	6.5	15.5	10.3	5.5	10.3	7.4	4.8	6.3	2.8	1.3	10.3	6.1	3.9	7.8	6.5	3.3
13.8	8.6	4.1	14.3	8.1	4.4	13.8	7.9	3.3	8.0	6.3	6.6	15.3	8.3	4.1	14.8	15.3	16.5
5.0	9.4	8.9	1.1	5.8	4.6	−1.9	5.4	6.7	1.9	3.2	3.3	0.5	6.7	5.5	10.1	5.9	2.5
3.6	7.4	7.1	5.2	8.3	6.2	−0.3	5.6	5.7	−1.4	4.3	4.7	4.4	7.8	5.7	11.8	8.2	5.0
8.8	10.9	8.6	4.9	6.9	4.0	1.9	5.4	4.6	−3.3	3.5	4.2	0.5	5.2	5.3	14.3	8.2	2.9
7.1	8.9	5.8	9.1	9.5	6.3	0.5	5.6	6.9	3.0	6.7	5.8	6.6	6.7	3.4	19.3	12.9	9.7
−0.6	8.6	8.4	−8.3	3.3	4.1	−8.3	3.1	3.9	−12.5	1.0	3.3	−9.6	3.3	4.5	16.2	2.4	−7.4
0.0	6.4	6.8	−9.9	7.4	12.9	−11.5	5.3	10.2	−14.4	1.4	4.7	−10.6	6.2	11.2	21.6	9.6	3.7
−9.9	7.0	11.8	−12.5	2.5	5.1	−12.2	4.5	8.9	−16.0	−0.4	2.4	−14.1	3.1	7.0	17.1	7.8	3.3
−6.4	5.8	6.6	−2.9	9.9	12.5	−10.3	6.6	11.4	−10.3	5.1	8.4	−6.7	6.4	8.5	24.3	10.2	3.3

Table 5. Concentration reductions inside bioassay cages at multiple air speeds and significance testing of air speed and cage orientation effects.

Cage	Tunnel air speed (m/s)	Average concentration reduction across both orientation angles, mean $\pm$ standard deviation (%)	Significance (* if significant) Air speed	Significance (* if significant) Orientation
CLA-84-D16	0.5	50.6 $\pm$ 10.8	* ($P < 0.001$)	($P = 0.2704$)
	2	33.9 $\pm$ 7.3		
	4	31.4 $\pm$ 7.8		
CSC-47-D16	0.5	100 $\pm$ 0.0	* ($P < 0.001$)	($P = 0.6651$)
	1	97.6 $\pm$ 2.8		
	2	77.8 $\pm$ 8.7		
	4	82.3 $\pm$ 7.3		
NEC-74-D9	0.5	66.0 $\pm$ 10.3	* ($P < 0.001$)	($P = 0.8483$)
	2	52.2 $\pm$ 7.0		
	4	41.4 $\pm$ 11.6		
NSC-47-D9	0.5	100 $\pm$ 0.0	* ($P < 0.001$)	($P = 0.2141$)
	1	99.0 $\pm$ 2.3		
	2	83.9 $\pm$ 6.0		
	4	78.6 $\pm$ 12.6		
WHO-72-C5	0.5	58.9 $\pm$ 15.4	* ($P = 0.1715$)	($P = 0.6875$)
	2	60.5 $\pm$ 22.6		
	4	48.5 $\pm$ 12.5		
PFB-58-C12	0.5	76.2 $\pm$ 11.8	* ($P = 0.0447$)	($P = 0.7732$)
	2	63.9 $\pm$ 11.8		
	4	63.5 $\pm$ 13.5		

linear relationship between spray penetration and the porosity of the screening material used (regardless of cage type) for each wind speed tested, with R^2 values of 0.95, 0.92, and 0.99 for air speeds of 0.5 m/sec, 2 m/sec, and 4 m/sec, respectively. Higher reductions were seen at lower air speeds and lower screen porosities. Both the Clarke and the NECE sand fly cages showed the least penetration of spray material, with essentially no material penetrating at the 0.5 m/sec and 1 m/sec air speeds. Based on the droplet sizing results, it is apparent that at least some fraction of spray penetrates at these air speeds, but the amounts were so minute that any material captured by the samplers was below the detection threshold of the spectrofluorophotometer. All cages showed greater penetration (i.e., less percentage reduction in concentration) of spray material at the higher air speeds.

DISCUSSION

A number of mosquito and sand fly bioassay cages were tested in low-speed wind tunnel studies to determine cage structure, size, and screening material effects on both air flow and spray droplet size penetrating the cages. Generally, air speed reductions were the greatest at lower external air speeds, with overall reductions ranging from 30% to 88%, depending on cage type and tunnel air speed. The reductions measured here are somewhat less at the lower air speeds than those reported by Hoffmann et al. (2008) because of the different anemometers used. The anemometers used for this work have a much

lower-end operational threshold and higher sampling rates than those used by Hoffmann et al. (2008), which were operating at the lower end of the operational threshold of the instruments (0.1 m/sec) during the low air speed testing.

Spray concentration reductions ranged from 32% to 100%, depending on the cage geometry, screening material, and external air speed observed. Face orientation relative to the mean air flow direction was not a significant factor, other than for a few cases, in the reduction of air speed, droplet size, or spray concentration. Screens with lower porosities, smaller cage types, and cylindrical cages tended to provide greater resistance to air flow and spray material. However, cylinder cages are beneficial in a field research environment where drastic changes in wind direction are common. A 90° change in wind direction on a disc cage would result in the flow field carrying spray droplets to impact the impenetrable sidewall. Additionally, cylinder cages with open mesh tops enable the entry of spray the sediments over the cage.

The results of this study have 2 main implications. The first is that accurate wind speeds need to be recorded during spray trials. Wind speed is often reported as ranging from <2.9 to 10 miles per hour (<0.9–4.5 m/s) and averaging about 4 mph (1.8 m/s) (Mount and Pierce 1972). With this level of variability, one would expect to see only large variances in the levels of control due to the significant differences of spray penetration into a bioassay cage at a wind speed of 0.9 m/s versus 4.5m/s. Additionally, researchers working in cage trials where air speed drops below 2 m/s

should anticipate that very little or no pesticide spray will penetrate into the cages.

The second implication is related to the practice of using bioassay cages to determine the effective minimum insecticide application rate. If the optimal dose of a particular insecticide was determined to be 1 oz/acre based on bioassay cage mortality studies, a more accurate ''optimal dose'' may in fact be lower due to reduced levels of spray material that actually penetrate into the cage. This ''optimal dose'' determined could vary by cage type and environmental conditions observed during the spray trials. Therefore, as reported by Geery et al. (1983), the rate observed in caged mosquitoes does not necessarily reflect that of a natural, dynamic population. Boobar (1988) also concluded that the interaction of mesh and spray would lead to an increase in observed mortality because of spray deposition on the mesh and the resulting tarsal exposure. More recently, Bonds et al. (2010), found that the predominant exposure mechanism was a space spray, or the amount of spray material that penetrated through the mesh, but the combined effect of space spray and residual tarsal contact showed a significant increase in mosquito mortality after 30 min, compared to space spray alone. The results presented in the our manuscript will aid comparisons between treatment data conducted under different wind speeds and studies conducted using different bioassay cage designs by providing a better understanding of how much spray material actually enters the cage.

ACKNOWLEDGMENTS

REFERENCES CITED

ASTM [American Society for Testing and Materials]. 2003. Standard E 1260: standard test method for determining liquid drop size characteristics in a spray using optical nonimaging light-scattering instruments. In: *Annual book of ASTM standards*. West Conshohocken, PA: American Society for Testing and Materials International.

ASTM [American Society for Testing and Materials]. 2004. Standard E 1620: standard terminology relating to liquid particles and atomization. In: *Annual book of ASTM standards*. West Conshohocken, PA: American Society for Testing and Materials International.

Barber JAS, Greer MJ, Coughlin J. 2006. The effect of pesticide residue on caged mosquito bioassays. *J Am Mosq Control Assoc* 22:469–472.

Bonds JAS, Greer M, Coughlin J, Venit P. 2010. Caged mosquito bioassay: studies on cage exposure pathways, effects of mesh on pesticide filtration, and mosquito containment. *J Am Mosq Control Assoc* 26:50–56.

Bonds JAS, Greer MJ, Fritz BK, Hoffmann WC. 2009. Aerosol sampling: comparison of two rotating impactors for field droplet sizing and volumetric measurements. *J Am Mosq Control Assoc* 25:474–479.

Boobar LR, Dobson SE, Perich MJ, Darby WM, Nelson JH. 1988. Effects of screen materials on droplet size frequency distribution of aerosols entering sentinel mosquito exposure tubes. *Med Vet Entomol* 2:379–384.

Breeland SG. 1970. The effect of test cage materials on ULV malathion evaluations. *Mosq News* 30:338–342.

Bunner BL, Posa SG, Dobson SE, Broski FH, Boobar LR. 1989. Aerosol penetration relative to sentinel cage configuration and orientation. *J Am Mosq Control Assoc* 5:547–551.

Cooper JF, Smith DN, Dobson HM. 1996. An evaluation of two field samplers for monitoring spray drift. *Crop Prot* 15:249–257.

Fox RD, Derksen RC, Zhu H, Downer RA, Brazee RD. 2004. Airborne spray collection efficiency of nylon screens. *Appl Eng Agric* 20:147–152.

Fritz BK, Hoffmann WC. 2008a. Collection efficiency of airborne spray flux samplers. *J Am Soc Test Mater Int* 5:1–10.

Fritz BK, Hoffmann WC. 2008b. Development of a system for determining collection efficiency of spray samplers. *Appl Eng Agric* 24:285–293.

Geery PR, Holub RE, Keen RR. 1983. Statistical evaluation of ground applied ULV malathion on natural populations of *Aedes vexans* and *Culex* species. *Mosq News* 43:206–208.

Hoffmann WC, Fritz BK, Farooq M, Cooperband MF. 2008. Effects of wind speed on aerosol spray penetration in adult mosquito bioassay cages. *J Am Mosq Control Assoc* 24:419–426.

Hoffmann WC, Hewitt AJ. 2005. Comparison of three imaging systems for water-sensitive papers. *Appl Eng Agric* 21:961–964.

Hoffmann WC, Walker TW, Martin DE, Barber JAS, Gwinn T, Szumlas D, Lan Y, Smith VL, Fritz BK. 2007. Characterization of truck mounted atomization equipment typically used in vector control. *J Am Mosq Control Assoc* 23:321–329.

Kosmos SR, Riskowski GL, Christianson LL. 1993. Force and static pressure resulting from air flow through screens. *Trans Am Soc Agic Biol Eng* 36:1467–1472.

May KR, Clifford R. 1967. The impaction of aerosol particles on cylinders, spheres, ribbons, and discs. *Ann Occup Hyg* 10:83–95.

Miguel AF. 1998. Air flow through porous screens: from theory to practical considerations. *Energy Build* 28:63–69.

Miller PCH. 1993. Spray drift and its measurement. In: Mathews GA, Hislop FC, eds. *Application technology for crop protection*. Wallingford, United Kingdom: CAB International. p 101–122.

Mount GA, Pierce NW. 1972. Adult mosquito kill and droplet size of ultralow volume ground aerosols of insecticides. *Mosq News* 32:354–357.

Teitel M. 2009. Using computational fluid dynamics simulations to determine pressure drop on woven screens. *Biosystems Engr* 105:172–179.